Highly Efficient Heterogeneous Photooxidation of 2-Propanol to Acetone with Amorphous Manganese Oxide Catalysts

Hui Cao[†] and Steven L. Suib*[,†,‡,§]

Contribution from the Department of Chemistry, U-60, Institute of Materials Science, and Department of Chemical Engineering, University of Connecticut, Storrs, Connecticut 06269-3060

Received October 26, 1993[⊗]

Abstract: Amorphous manganese oxides, potassium oxalatomanganate complexes, and crystalline tunnel structure manganese oxides (hollandite, todorokite, pyrolusite) have been prepared and used as photocatalysts for the oxidation of 2-propanol to acetone. Amorphous mixed valent manganese oxides, a new class of photocatalytic materials, were the most active catalysts studied at room temperature under visible light illumination. High activities correlate with higher oxidation state manganese (Mn^{3+}, Mn^{4+}) oxides, large surface oxygen concentrations, and the presence of hydroxyl groups on surfaces of these catalysts. BET (surface area analysis), XRD (X-ray diffraction), EDX (energy dispersive X-ray analysis), SEM (scanning electron microscopy), XPS (X-ray photoelectron spectroscopy), and FTIR (Fourier transform infrared) data support these correlations. A mechanism for these photooxidation flow reactions involving manganese oxide catalysts has been proposed. Photochemical and characterization data suggest that the design of active photocatalysts may rely on preparation of mixed valent amorphous oxides that release oxygen more readily than crystalline materials. Conversions as high as 8% and 100% selectivity to acetone have been realized with such systems.

I. Introduction

Manganese oxide is used in dry cell batteries, in ferrite production, as an oxidizing agent in organic synthesis, as a cross-linking agent in rubber, and as a component of oxidation catalysts.[1] When MnO_2 is used as an oxidizing agent in organic reactions, stoichiometric amounts of MnO_2 are used. Rates of allylic and benzylic alcohol oxidation over MnO_2 are typically faster than over saturated aliphatic alcohols.[2] Radical intermediates have been proposed in such reactions.[3] In certain cases, overoxidation of aldehydes to esters or carboxylic acids can be carried out with MnO_2.[4]

Manganese is an essential component in photosynthetic systems.[5-9] Water-splitting reactions can also be catalyzed by manganese.[6,7] Manganese is known to be a necessary element in many biological systems, and its reduction–oxidation chemistry is especially important in electron-transfer reactions.[8,10-13] Reactions that mimic biological systems in order to utilize solar energy have often focused on manganese catalysts; however, activity is low. To understand the role of the manganese cofactor in biological electron-transfer reactions, model studies of the photochemistry of various manganese complexes may be fruitful. Unfortunately, there are relatively few manganese complexes that have long-term photochemical stability. This has provided impetus for the preparation of various manganese compounds that are stable and that have photoredox functions that might be used to catalyze photochemical reactions.

There have been several recent photochemical and photocatalytic studies of zeolites, clays, pillared clays, and molecular sieve materials.[14] Photocatalytic studies have focused on tryptophan photooxidation,[15] artificial photosynthesis,[14c,16] rearrangement and disproportionation of alkyl dibenzyl ketone,[17] and Norrish type I and II reactions of benzoin[18] and dibenzyl ketones.[19] The latter studies have shown that slurry systems are more selective than dry solid systems. Some unanswered questions in all these studies include procedures for choosing photocatalysts that are appropriate for different reactions, what role structure plays in catalytic activity and selectivity, and what are optimal conditions for carrying out such experiments (static vs flow reactor, slurry vs solid, etc.).

Although manganese dioxide is a well-known oxidant and has been successfully used as a catalyst for thermally catalyzed reactions,[20,21] we are not aware of studies of manganese oxide

* Author to whom correspondence should be addressed.
† Department of Chemistry.
‡ Institute of Materials Science.
§ Department of Chemical Engineering.
⊗ Abstract published in *Advance ACS Abstracts,* May 15, 1994.

(1) (a) Buchner, W.; Schliebs, R.; Winter, B.; Buchel, K. H. *Industrial Inorganic Chemistry*; VCH: Weinheim, 1989; pp 281–286. (b) Li, K. T.; Peng, Y. J. *J. Catal.* **1993**, *143*, 631–634.
(2) Nickon, I.; Bagli, J. F. *J. Am. Chem. Soc.* **1961**, *83*, 1498–1508.
(3) Goldman, I. M. *J. Org. Chem.* **1969**, *34*, 3289–3295.
(4) (a) Woo, E. P.; Sondheimer, F. *Tetrahedron* **1970**, *26*, 3933–3939. (b) Yamamoto, K.; Sondheimer, F. *Angew. Chem., Int. Ed. Engl.* **1973**, *12*, 68–69.
(5) Koulougliotis, D. H.; Donald, J.; Brudvig, G. W. *J. Am. Chem. Soc.* **1992**, *114*, 8322–8323.
(6) Hall, D. O.; Rao, K. K. *Photosynthesis* (Studies in Biology No. 37, 2nd ed.); Edward Arnold Publ.: London, 1977.
(7) Tennakone, K.; Tantrigoda, R.; Abeysinghe, S.; Punchihewa, S.; Fernando, C. A. N. *J. Photochem. Photobiol. A: Chem.* **1990**, *52*, 43–46.
(8) Libby, E.; McCusker, J. K.; Schmitt, E. A.; Folting, K.; Hendrickson, D. N.;Christou, G. *Inorg. Chem.* **1991**, *30*, 3486–3495.
(9) (a) Wang, S.; Folting, K.; Streib, W. E.; Schmitt, E. A.; McCusker, J. K.;Hendrickson, D. N.; Christou, G. *Angew. Chem.* **1991**, *103*, 305–306. (b) Wang, S.; Folting, K.; Streib, W. E.; Schmitt, E. A.; McCusker, J. K.;Hendrickson, D. N.; Christou, G. *Angew. Chem.* **1991**, *103*, 314–316.
(10) Pick, M.; Rabani, J.; Yost, F.; Fridovich, I. *J. Am. Chem. Soc.* **1974**, *96*, 7329–7333.
(11) Edwards, G.; Walker, D. In *Mechanisms, and Cellular and Environmental Regulation, of Photosynthesis*, University of California Press: Berkeley and Los Angeles, 1983; p 64.
(12) De Paula, J. C.; Beck, W. F.; Brudvig, G. W. *J. Am. Chem. Soc.* **1986**, *108*, 4002–4009.
(13) Beck, W. F.; De Paula, J. C.; Brudvig, G. W. *J. Am. Chem. Soc.* **1986**, *108*, 4018–4022.
(14) (a) Turro, N. J. *Pure Appl. Chem.* **1986**, *58*, 1219–1224. (b) Ramamurthy, V. In *Inclusion Phenomena and Molecular Recognition*; Atwood, J., Ed.; Plenum Press: New York, 1990; pp 351–363. (c) Krueger, J. S.; Mallouk, T. E. In *Kinetics and Catalysis in Microheterogeneous Systems*; Gratzel, M., Kalyanasundaram, K., Eds.; Marcel Dekker: New York, 1991; pp 461–490. (d) Suib, S. L. *Chem. Rev.* **1993**, *93*, 803–826.
(15) Cenens, J.; Schoonheydt, R. A. *Clay Miner.* **1988**, *23*, 205–212.
(16) Krueger, J. S.; Lai, C.; Li, Z.; Mayer, J. E.; Mallouk, T. E. In *Inclusion Phenomena and Molecular Recognition*; Atwood, J., Ed.; Plenum Press: New York, 1990; pp 365–378.
(17) Ramamurthy, V.; Corbin, D. R.; Eaton, D. F. *Tetrahedron Lett.* **1989**, *30*, 5833–5836.
(18) Corbin, D. R.; Eaton, D. F.; Ramamurthy, V. *J. Am. Chem. Soc.* **1988**, *110*, 4848–4849.
(19) Ramamurthy, V.; Corbin, D. R.; Turro, N. J.; Zhang, Z.; Garcia-Garibay, M. A. *J. Org. Chem.* **1991**, *56*, 255–261.

0002-7863/94/1516-5334$04.50/0

Table 1. Turnover Rates and Surface Areas of Photocatalysts for 2-Propanol to Acetone Conversion over Amorphous Manganese Oxide Catalysts

	surface area[a]	turnover rate[b]
A-MnO_2[c]	164	1.655×10^{-3}
B-MnO_2[d]	335	6.09×10^{-4}
C-MnO_2	349	3.31×10^{-4}
D-MnO_2	333	6.027×10^{-4}
commercial MnO_2[e] (<80 μm)	42	1.552×10^{-3}
commercial MnO_2[e] (>80 μm)	1	5.74×10^{-5}

[a] In m^2/g. [b] In mol acetone/h g catalyst. [c] Mn/K = 16.4 by EDX. [d] Mn/K = 15.0 by EDX. [e] No K detected.

species as photocatalysts. This paper describes photoassisted catalytic oxidation reactions over a variety of manganese oxide materials including synthetic tunnel structure materials,[22,23] crystalline oxalate manganese complexes, and newly developed amorphous materials. The turnover number for the most active catalyst is 5–6 times higher than the best uranyl oxide and zeolite catalysts we have studied[27] and 500–600 times higher than previous static liquid phase reactions on uranyl aluminosilicate catalysts.[24-26] Selectivity to acetone can be as high as 100% with overall conversions of 8%.

II. Experimental Section

A. Preparation of Manganese Catalysts. Hollandite,[27,28] todorokite,[22,23] pyrolusite,[28] and potassium oxalatomanganate complexes [$(Mn(C_2O_4)_3]$,[29,30] $[Mn(C_2O_4)_2]$, $[Mn(C_2O_4)OH]$,[29,30] or $[Mn(C_2O_4)(OH)_2]$[29,30] were prepared by literature methods.[22,23,27-30] The amorphous manganese oxides were prepared by the reaction of potassium permanganate with oxalic acid or manganese(2+) acetate. The precipitated manganese oxides were washed with distilled deionized water and vacuum dried.

Amorphous MnO_2 (A-MnO_2) was prepared by the reduction of 1.58 g of potassium permanganate dissolved in 60 mL of DDW with 2.28 g of oxalic acid dissolving in 100 mL of DDW. Similar amorphous materials (B-MnO_2) were prepared the same way, except with a ratio of 1.58 g of potassium permanganate to 1.78 g of oxalic acid. Another amorphous material, C-MnO_2, was prepared by reduction of 1.58 g of potassium permanganate with 3.68 g of manganese(2+) acetate. A final material (D-MnO_2) was prepared in the same way, the ratio of which is 1.58 g of potassium permanganate to 9.80 g of manganese(2+) acetate. Some physical properties of A-MnO_2 and potassium oxalatomanganate are summarized in Table 1.

B. Photocatalysis Experiment. About 0.025 g of manganese oxide catalyst with 0.025 g of support (MgO) were well mixed and loaded into a sealed reactor. Light was reflected into the reactor by a concave mirror (Figure 1). The light beam was focused on the window of the reactor (2.7 cm in diameter), and the catalyst was spread as a thin layer inside the in situ stainless steel reactor. A carrier gas (O_2) was passed through a bubbler containing 2-propanol, which was transported into the reactor by the carrier gas.

The light source for irradiation of the catalyst and organic reactant was a 1000-W continuous output Xe arc lamp. The light was passed first through a bottle of distilled water to absorb infrared radiation and then through a 425-nm cutoff filter to allow only visible light into the reactor. The catalytic reaction products were condensed in a dry ice/acetone cold trap and were syringed into a gas chromatograph for analysis. Use of liquid nitrogen traps for CO_2 and on line analyses for CO do not show production of either CO or CO_2.

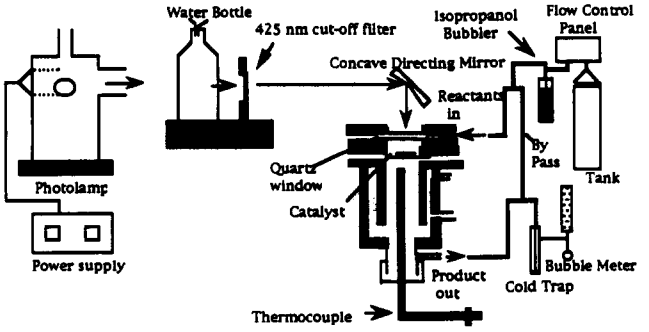

Figure 1. Diagram of photocatalytic reactor.

C. Gas Chromatographic Analyses. Gas chromatographic (GC) analyses of the photolyzed mixtures were performed on a Hewlett-Packard Model 5880A system equipped with a thermal conductivity detector set at 250 °C. One-microliter solutions were injected into the column. The helium carrier gas was set at 30 cm^3/min. The injector temperature was set at 250 °C, and the oven temperature was 100 °C. The column used for separation was a 10% Carbowax 20 M on 60-80 mesh Anakrom on C-22 firebrick.

D. X-ray diffraction (XRD). X-ray diffraction data were collected by using a Scintag Model PDS-2000 diffractometer. Samples were loaded onto glass slides, and Cu Kα radiation was used at 45 kV and 40 mA. The sample scans were done at 2°2θ/min. Several amorphous manganese oxides were scanned at 0.5°2θ/min.

E. Energy Dispersive X-ray Analysis (EDX). An AMRAY/LICO energy dispersive X-ray (EDX) analyzer Model 9800 was used for EDX studies. An average of five to eight analyses were done to determine average concentrations of chemical components.

F. X-ray Photoelectron Spectroscopy (XPS) Analysis. A Leybold-Heraeus Model LHS-10 X-ray photoelectron spectrometer with Mg Kα radiation was used to study the binding energies of elements of the catalysts with a pass energy of 150 eV. The anode was operated at 12 kV and 20 mA. Survey scans over the kinetic energy range 300–1300 eV and selected narrow region scans for the elements K, Mn, and O were done.

G. Surface Area Analyses (BET). Analyses of surface areas (BET) were done using an OMNISORP-100CX analyzer. Prior to adsorption at 78 K with liquid nitrogen, samples were outgassed at several temperatures (up to 350 °C).

Sorption was carried out under a continuous flow. At each sample point, the gas was in equilibrium with the adsorbed phase and an equilibrium isotherm of over 1000 data points was collected. Adsorption isotherms (a plot of $P/V_{ads}(P_0 - P)$ vs P/P_0) and BET calculations were done with OMNISORP software.

H. Thermal Analyses. The thermal properties of the different catalysts were studied by differential scanning calorimetry (DSC) (DuPont Model 9900) and by thermogravimetric analysis (TGA). Samples were heated to 600 or 1000 °C in oxygen or nitrogen atmospheres with a flow of 20 mL/min. The rate was 5 or 10 °C/min.

I. Fourier Transform Infrared Spectra (FTIR). The FTIR experiments in the mid IR region were done on a Nicolet SX-60 FTIR instrument equipped with a triglycine sulfate (TGS) detector with a KBr window and a KBr beam splitter and were purged with dry air to prevent interference from atmospheric moisture. Transmission FTIR spectra were obtained with a resolution of 4 cm^{-1} by using 32 scans. The powdered samples were diluted with finely ground KBr to about 1–5% by weight. Far-infrared data were collected with a TGS detector with a polyethylene window and a silicon beam splitter.

III. Results

A. Properties and Structures of Manganese Oxides and Complexes. Pure potassium oxalatomanganate, crystalline manganese oxides (todorokite, hollandite, pyrolusite), and amorphous manganese oxides were prepared and characterized by IR, XRD, SEM, XPS, and BET. Separation of potassium oxalatomanganate complexes and manganese oxides was done by using different solvents since manganese oxides preferentially precipitate in aqueous solution, but potassium oxalatomanganate complexes have a greater solubility in aqueous solution and precipitate well

(20) Nitta, M. *Appl. Catal.* **1984**, *9*, 151–176.
(21) (a) Kobayashi, M.; Matsumoto, H.; Kobayashi, H. *J. Catal.* **1971**, *21*, 48–55. (b) Jiang, S. P.; Ashton, W. R.; Tseung, A. C. C. *J. Catal.* **1991**, *131*, 88–93.
(22) Shen, Y. F.; Zerger, R. P.; Suib, S. L.; McCurdy, L.; Potter, D. I.; O'Young, C. L. *J. Chem. Soc., Chem. Commun.* **1992**, *17*, 1213–1214.
(23) Shen, Y. F.; Zerger, R. P.; DeGuzman, R. N.; Suib, S. L.; McCurdy, L.; Potter, D. I.; O'Young, C. L. *Science* **1993**, *260*, 511–515.
(24) Suib, S. L; Tanguay, J. F.; Occelli, M. L. *J. Am Chem. Soc.* **1986**, *108*, 6972–6977.
(25) (a)Suib, S. L; Kostapapas, A.; Psaras D. *J. Am. Chem. Soc.* **1984**, *106*, 1614–1620. (b)Eaton, M. E.; Stuart, J. D. *Anal. Chem.* **1978**, *50*, 587–591.
(26) Suib, S. L; Carrado K. A. *Inorg. Chem.* **1985**, *24*, 863–867.
(27) Tsuji, M.; Abe, M. *Solvent Extr. Ion Exch.* **1984**, *2*, 253–274.
(28) O'Young, C. L. In *Synthesis of Microporous Materials*; Occelli, M., Robson, H., Eds.; van Nostrand Reinhold: New York, 1992; Vol. II, pp 333–340.
(29) Cartledge, G. H.; Erick, W. P. *J. Am. Chem. Soc.* **1936**, *58*, 2069–2072.

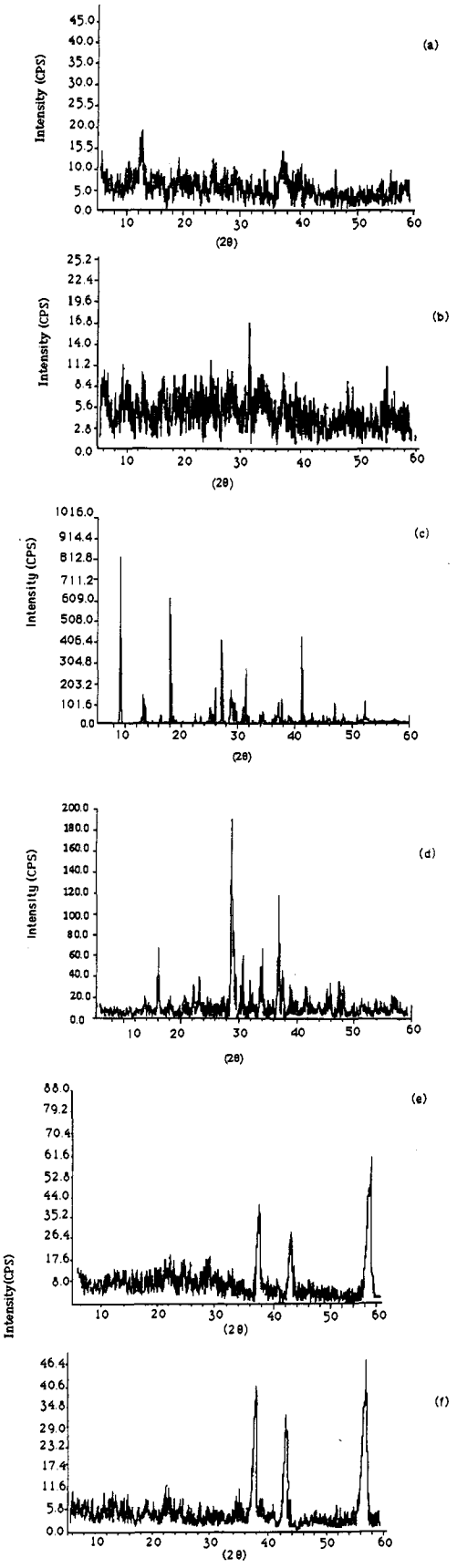

Figure 2. XRD patterns of manganese oxides and potassium oxalatomanganate: (a) fresh A-MnO_2; (b) photolyzed A-MnO_2; (c) fresh potassium oxalatomanganate; (d) photolyzed potassium oxalatomanganate; (e) fresh commercial MnO_2; (f) photolyzed commercial MnO_2.

in alcohol.[29,30] The XRD patterns of all manganese oxide materials are quite different (Figure 2).

The slow scan XRD data (Figure 2a,b) showed that the manganese oxide catalyst A-MnO_2 materials are amorphous powders with weak peaks at 6.9 and 2.4 Å. Similar patterns were observed for B-MnO_2, C-MnO_2, and D-MnO_2. The fresh potassium oxalatomanganate complexes have sharp and high intensity diffraction peaks (Figure 2c), indicating well formed crystalline material. After these complexes are exposed to light of 425 nm with 700-W power for about 2 h, the XRD pattern changed to a completely different pattern, with loss of diffraction peaks at high d spacings (Figure 2d). The commercial MnO_2 catalyst has a weak diffraction pattern with d spacings of 2.4, 2.1, and 1.62 Å (Figure 2e,f).

The amorphous manganese oxides are quite stable in light and regenerable in an oxygen atmosphere. The corresponding photolyzed amorphous catalysts showed very similar XRD patterns with loss of only some physisorbed or chemisorbed water, as evidenced by thermogravimetry studies (vide infra) as shown for A-MnO_2 in Figure 2a,b.

B. Photocatalytic Activities of Manganese Oxide Catalysts. Various manganese oxides, such as hollandite, todorokite, pyrolusite, amorphous manganese oxides, and commercial manganese dioxide, were used as photocatalysts for the oxidation of 2-propanol to acetone and showed very different catalytic activities (Figure 3). The turnover rates of various amorphous manganese oxides decreased in the order A-MnO_2 > MnO_2 (commercial) > B-MnO_2 > C-MnO_2 > D-MnO_2 (Table 1). The selectivity of these catalysts can be as high as 100% at room temperature. On the other hand, the crystalline manganese oxides such as hollandite, todorokite, and pyrolusite and large particles (70–80 μm) of commercial crystalline manganese oxide showed very poor photocatalytic activities. Pure $MnSO_4$ showed no activity for photooxidation. Surface areas for MnO_2 catalysts are also given in Table 1.

An aging study showed that the turnover number of catalyst A-MnO_2 remained the same even after 72 h of reaction. No acetone was produced in the absence of manganese oxide under light illumination. The photolyzed MgO support itself is also inactive for the oxidation of 2-propanol.

C. Role of Light. Figure 4 shows that as the incident power is increased, the rate of formation of acetone increases for catalyst A-MnO_2. Corresponding dark experiments showed 10–20 times lower conversions than those of the most active commercial manganese dioxide catalysts. Plots of yields of acetone for dark reactions and for power levels of 700 W are given in Figure 5 for catalyst A-MnO_2.

D. Role of Oxygen Carrier Gas. Figure 6 shows a plot of the yield of acetone versus time for catalyst A-MnO_2 photolyzed in oxygen,[6] prephotolyzed in O_2, and prephotolyzed in nitrogen. The fresh A-MnO_2 catalyst treated with an oxygen flow rate of 27.3 mL/min and power of 700 W showed a high stable activity (Figure 6). Photolysis of the catalyst in an oxygen-free atmosphere for about 1 h prior to reaction with 2-propanol led to a loss of 90% of the original activity (Figure 6). This catalyst lost all activity soon after this first hour of photolysis. Photolysis with an oxygen flow rate of 27.3 mL/min (photolyzed about 1 h prior to reaction with 2-propanol) led to a conversion of 68% of the original activity (Figure 6). These results provide information that oxygen carrier gas is necessary during reaction for facile regeneration of the catalysts.

E. Nature of Active Sites. (1) Chemical Composition (EDX and XPS). The EDX (Table 1) and XPS data (Figure 7) show that the main elements of the most active amorphous manganese oxide catalyst (A-MnO_2) consist of potassium, manganese, oxygen, trace amounts of carbon, and chlorine. Valence band spectra for commercial MnO_2 before and during photolysis in the XPS instrument are shown in Figure 7, parts a and b, respectively. The bands near 20 eV are due to oxygen, whereas those near 50 eV are due to manganese. After photolysis it is clear that the O/Mn ratio has markedly increased. Similar results are observed for A-MnO_2. Binding energies of 665.48 and 653.42 eV for the Mn $2p_{1/2}$ transitions and 641.96 eV for the Mn $2p_{3/2}$ transition

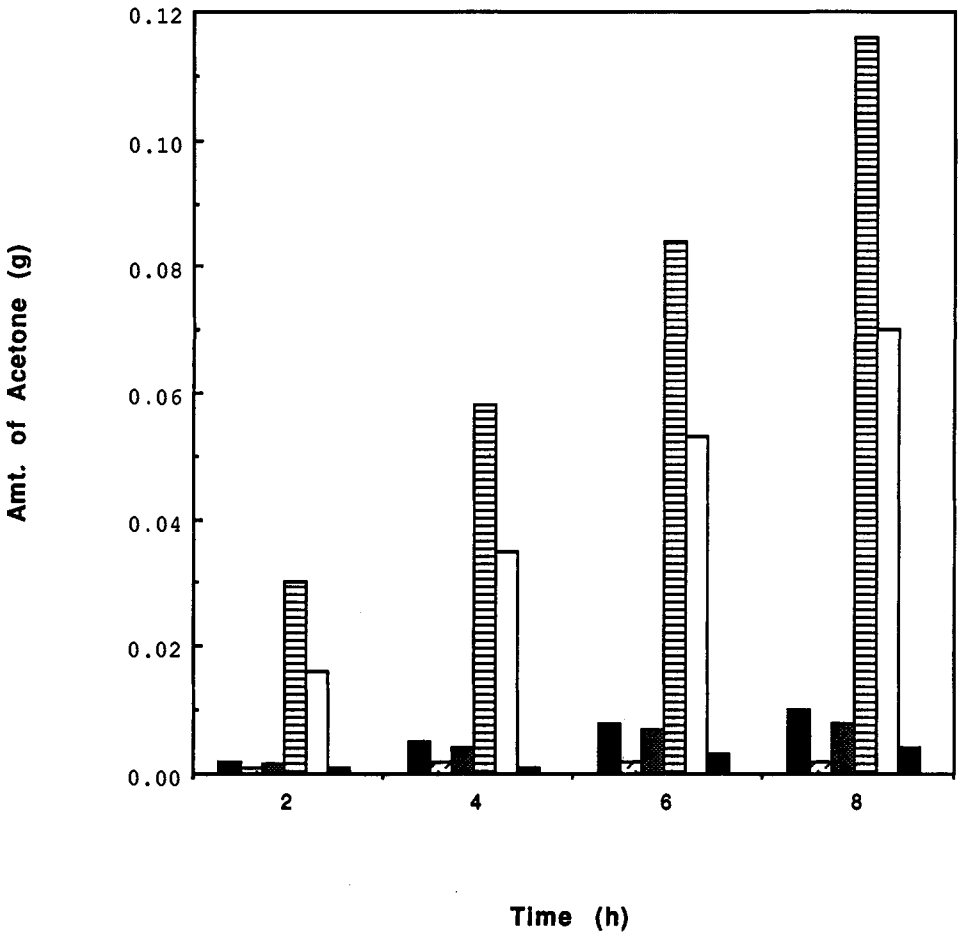

Figure 3. Yields for manganese oxide catalysts at 2, 4, 6, and 8 h from left to right: hollandite; cryptomelane; todorokite; A-MnO_2; commercial A-MnO_2 (<80 μm); commercial A-MnO_2 (>80 μm).

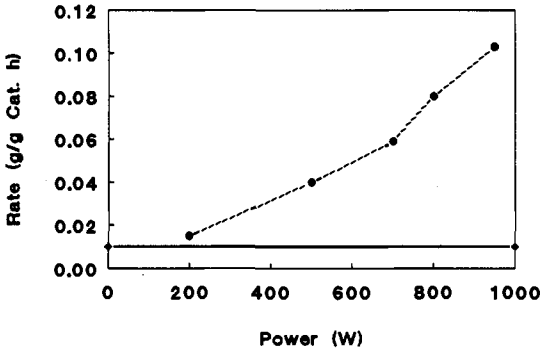

Figure 4. Relation of rate versus power level for A-MnO_2.

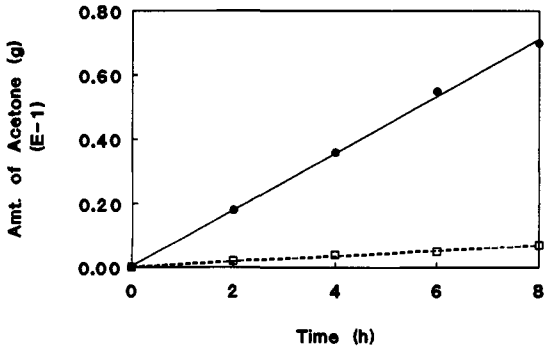

Figure 5. Effect of incident power on yields of acetone for A-MnO_2: (□) dark reaction; (●) 700 W.

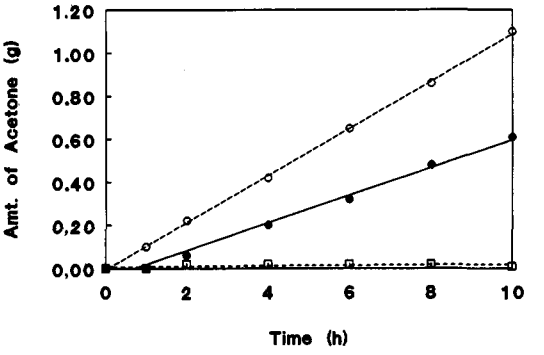

Figure 6. Effect of prephotolysis and oxygen on manganese oxide catalysts: (○) fresh catalyst photolyzed in oxygen; (●) prephotolyzed 1 h in O_2; (□) prephotolyzed 1 h in N_2.

are indicative of a mixed valent manganese system, most likely due to Mn(4+) and Mn(3+). The XPS data for commercial manganese dioxide show binding energies of 653.31 for Mn $2p_{1/2}$ and 641 eV for Mn $2p_{3/2}$, indicative of Mn(4+). No impurity cations were observed with XPS. Comparisons of XPS, EDX, and ion-scattering data suggest that K^+ is evenly distributed throughout A-MnO_2.

(2) Thermal Analyses. The thermal stabilities of potassium oxalatomanganate complexes and amorphous manganese oxides are quite different. Upon heating the potassium oxalatomanganate complexes, a color change (similar to that observed under light irradiation) was observed from 75 to 100°C. Heating A-MnO_2 and commercial manganese dioxide at 100 °C for about 5–10 h did not result in any color change.

Two major weight changes were found in the TGA curves for the amorphous manganese oxide catalyst A-MnO_2, as shown in Figure 8a. The first weight loss, from about 50 to 170 °C corresponds to dehydration of both physisorbed and chemisorbed

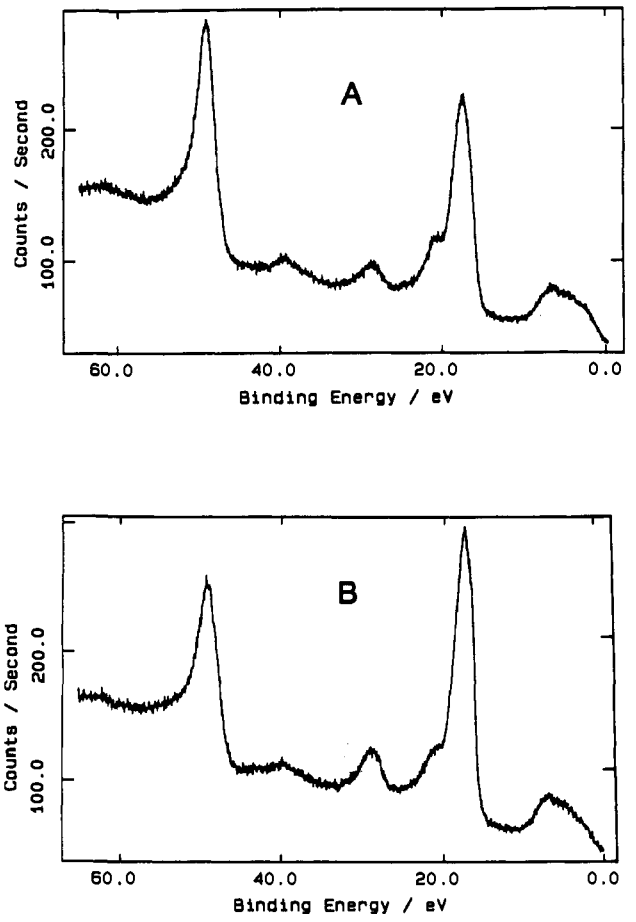

Figure 7. Valence band X-ray photoelectron spectra of (A) A-MnO_2 and (B) A-MnO_2 photolyzed in an XPS instrument.

water and adsorbed surface oxygen molecules (vide infra).[31] The second weight loss at 240–250 °C may be due to decomposition and calcination of excess oxalic acid and trace amounts of potassium oxalatomanganate complexes.

The endothermic peak in the differential scan calorimetry (DSC) curve of A-MnO_2 begins at 40 °C and contains a superimposed exothermic peak with a DT_{max} (derivative temperature maximum) of 85 °C, while a second endothermic reaction occurs at 130 °C, as seen in Figure 8b. These two endothermic reactions are assigned to the loss of hydrate-bound water and surface oxygen,[31] respectively. The exothermic peak between 225 and 275 °C may be due to the decomposition of oxalic acid or potassium oxalatomanganate complexes, although as a reviewer has pointed out, there is no obvious change in weight of the sample in this range. There is a small slope near 280 °C, probably due to the reduction of higher oxidation state manganese ions to lower oxidation states accompanied by further release of oxygen[31] from the sample.

The fresh A-MnO_2 catalyst has about 15 wt % of H_2O, oxalic acid, or potassium oxalatomanganate species, which are evolved when heated above 100 °C. The fresh commercially active manganese dioxide catalysts have a composition of 95 wt % pure MnO_2 and 5% water. There is a large weight loss at 550–600 °C in the TGA curve for the commercial catalyst, Figure 8c. DSC data for the commercial MnO_2 catalyst (Figure 8d) also show a large endothermic peak in this temperature region. This is likely due to the reduction of manganese(IV) species to lower oxidation states[22,23] associated with loss of bulk oxygen.[31] There is an endothermic peak at 50 °C in the DSC data and some

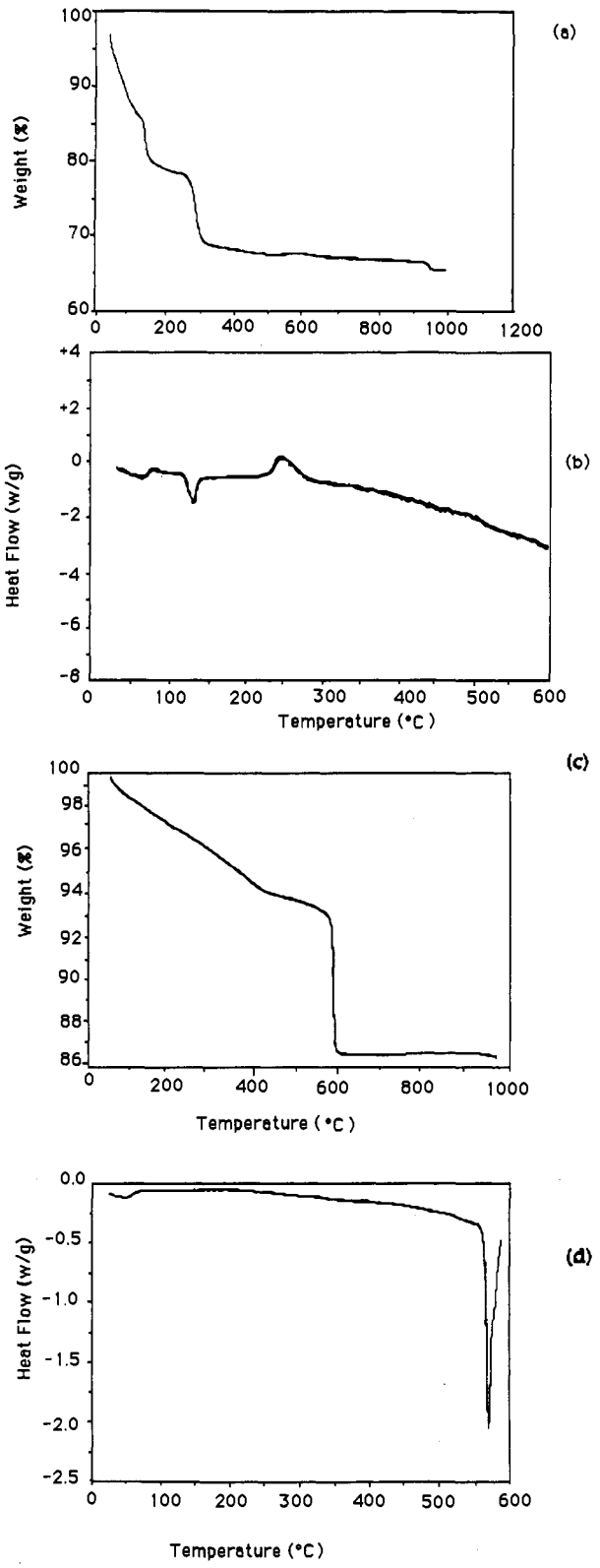

Figure 8. Thermal analyses of manganese oxide catalysts: (a) TGA of A-MnO_2; (b) DSC of A-MnO_2; (c) TGA of commercial A-MnO_2; (d) DSC of commercial A-MnO_2.

(30) Cartledge, G. H.; Erick, W. P. *J. Am. Chem. Soc.* **1936**, *58*, 2061–2065.
(31) Kung, H. *Transition Metal Oxides: Surface Chemistry and Catalysis*; Elsevier: Amsterdam, 1989; pp 100–120.
(32) Kon, M. Ya.; Shvets, V. A.; Kazanskii, V. B. *Kinet. Katal.* **1972**, *13*, 650–655.
(33) Matsuura, I.; Schuit, G. C. A. *J. Catal.* **1971**, *20*, 19–39.
(34) Kon, M. Ya.; Shvets, V. A.; Kazanskii, V. B. *Dokl. Akad. Nauk. SSSR.* **1972**, *203*, 624–627.
(35) Cunningham, J.; Hodnett, B. K. *J. Chem. Soc., Faraday Trans. 1* **1981**, *77*, 2777–2801.
(36) Ollis, D. F.; Hsiao, C. Y.; Lee, C. L. *J. Catal.* **1983**, *82*, 418–423.
(37) Opportunities for Pollution Prevention Research to support the 33/50 Program, EPA/600/R-92/175, USEPA, Office of Research and Development, Washington, DC 20460, October 1992.
(38) Noda, M.; Shinoda, S.; Saito, Y. *Bull. Chem. Soc. Jpn.* **1988**, *61*, 901–956.
(39) Yamashita, M.; Kandmura, T.; Suzuki, M.; Saito, Y. *Bull. Chem. Soc. Jpn.* **1991**, *64*, 272–278.

weight loss in the TGA curve before 350 °C, due to dehydration and loss of surface adsorbed oxygen molecules and bulk oxygen.[31]

(3) Photolysis Studies. Photolysis (Table 1) and infrared (Figure 9) studies show that potassium oxalatomanganate complexes are decomposed while exposed to light. The dark red-violet color of oxalatomanganate complexes changed to white on irradiation with visible light of 425 nm after about 30 min. The A-MnO_2 and commercial manganese dioxide catalysts do not change their color during irradiation.

After in situ irradiation of commercial MnO_2 for about 30 min, an XPS spectrum was immediately collected. The amount of surface oxygen increased about 5.2 times after irradiation.

The A-MnO_2 catalyst which was prephotolyzed in oxygen flow (27.3 mL/min) for about 1 h followed by photocatalytic reaction (Figure 6b) showed a decrease in activity of about 32% as compared to the same catalyst photolyzed in oxygen (no prephotolysis). This diminished activity was maintained for over 24 h after the initial prephotolysis. The activity of commercial MnO_2 decreased by 90% when photolyzed for 1 h in an O_2-free environment.

These experimental results provide information regarding the role of surface oxygen in these photocatalytic reactions and in regeneration of the catalysts. In an oxygen-free atmosphere, the catalyst is unable to be regenerated, which leads to loss in activity. Photolysis in the absence of the MgO support leads to substantial (up to 10×) loss in activity.

The fresh amorphous MnO_2 sample A-MnO_2 is brown prior to irradiation at 425 nm and is stable when heated to 70–100 °C. It is insoluble in water and ethanol. Potassium oxalatomanganate complexes are purple-red and decompose either during photolysis at 425 nm or on heating to 70–100 °C. The complex is soluble in water and insoluble in ethanol. A-MnO_2 and commercial MnO_2 show no change in color nor large changes in structural properties. Potassium oxalatomanganate did change color on photolysis from purple-red to colorless, and the structure changed to a less crystalline material.

Turnover numbers for AMO have been calculated by assuming that all Mn^{x+} sites are active. This leads to minimum turnover numbers since it is not yet possible to tell which Mn^{x+} sites are active and which are not. AMO which is photolyzed with a lamp power of 752 W for 8 h produces 104.4 cycles of acetone; that is to say that 104.4 mol of acetone are produced for every mole of Mn^{x+} in this 8-h period. For purposes of comparison, about 6 mW of power at 425 nm is produced at the surface of AMO, as determined by literature procedures.[25]

(4) Surface Area Analysis (BET). Although the XRD patterns of fresh A-MnO_2, B-MnO_2, C-MnO_2, and D-MnO_2 are similar, their surface areas are not the same. Table 1 shows a comparison of surface areas and rates of formation of acetone for different catalysts. There is no direct relation between surface area and rate. These data suggest that efficient catalysts need isolated active centers to avoid quenching and diffusion in the regeneration process. Samples photolyzed in either oxygen or oxygen-free atmospheres show some decrease in surface area (<10% total area), indicating that some local structural damage or aggregation may occur during light illumination.

(5) Morphology and Particle Size Analysis (SEM). Scanning electron microscopy (SEM) data show that A-MnO_2 has a nondistinct morphology with most particles on the order of 0.3 μm. The particle sizes of the commercial manganese dioxide catalyst (1–2 μm) are 50–80 times smaller than the inert commercial manganese dioxide (100 mesh, 70–80 μm), revealing that more active catalysts have smaller particle sizes that may be necessary for light absorption, diffusion, regeneration, and diminished quenching effects.

(6) Fourier Transform Infrared Spectra (FTIR). Most of the infrared (IR) data (Figure 9) were collected on fresh catalysts in order to mimic real catalytic conditions because fresh catalysts were more active than heated or irradiated catalysts. IR data

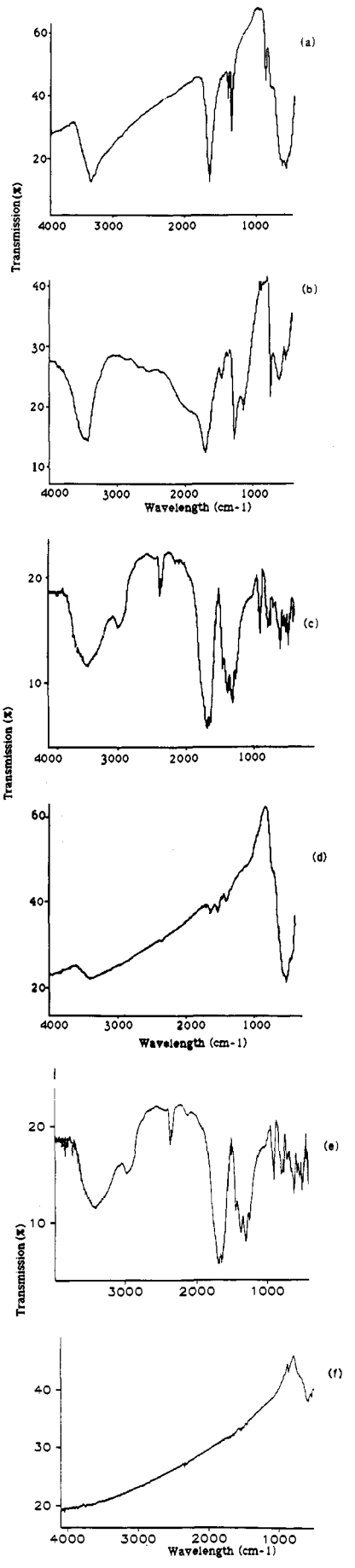

Figure 9. FTIR spectra of manganese oxide catalysts: (A) fresh A-MnO_2; (b) fresh $H_2C_2O_4$; (c) fresh potassium oxalatomanganate; (d) photolyzed A-MnO_2; (e) photolyzed potassium oxalatomanganate; (f) fresh commercial MnO_2.

were also collected on manganese oxides that were heated to 100 °C and evacuated to 10^{-2} Torr for 24 h for comparison.

IR data for fresh amorphous manganese oxide catalysts (A-MnO_2) in Figure 9a show the existence of excess oxalic acid, which has absorptions at 1623, 1635, and 1314 cm^{-1}, water absorption at 1600 and 3600 cm^{-1}, and hydroxyl groups around 3100–3600 cm^{-1}. Commercial oxalic acid has a similar IR pattern, as shown in Figure 9b. The potassium oxalatomanganate complexes have unique IR spectra, as seen in Figure 9c, with oxalate absorbances showing broad bands near 1625 and 1300 cm^{-1}. The photolyzed A-MnO_2 catalysts (Figure 9d) show drastic reductions in oxalate absorbance as compared to fresh A-MnO_2 (Figure 9a). The photolyzed potassium oxalatomanganate complexes (Figure 9e) show somewhat weaker absorption bands for oxalate ligands with respect to the fresh potassium oxalatomanganate (Figure 9c), indicating that potassium oxalatomanganate complexes and oxalic acid partially decompose on irradiation with visible light.

The IR patterns of the active commercial manganese dioxide catalysts (Figure 9f) do not have any absorption peaks in the regions where either oxalic acid or potassium oxalatomanganate complexes are located. The absorption intensity of water or OH^- groups on the active commercial manganese dioxide is much lower than those on the A-MnO_2 system. This appears to be the reason why the surface of A-MnO_2 is more acidic than the active commercial manganese dioxide. The existence of excess oxalic acid on fresh A-MnO_2 may allow more hydroxyl groups to be generated on the surface of A-MnO_2 during photolysis and alter the isoelectric point of the surface.

The water and hydroxyl bands at 3100–3600 and 1600 cm^{-1} as well as the oxalic acid bands at 1700–1600, 1405, and 1030 cm^{-1} become weaker after photolysis (Figure 9d,e), suggesting the loss of some physically adsorbed water and oxalic acid during photolysis.

After evacuation during heating at 100 °C for 24 h, the IR spectrum of A-MnO_2 showed weaker oxalic acid and water absorptions, indicating that most of the oxalic acid decomposes. However, some hydroxyl groups still remained on the surface. These surface hydroxyl groups are due to either adsorbed water or oxygen present during the photocatalytic reaction. A hydrogen abstraction mechanism involving hydroxyl groups may be important in these systems (vide infra). Heating and photolysis destroyed some of these hydroxyl groups with a concomitant decrease in photocatalytic activity (Figure 6).

(7) Further Characterization Studies of A-MnO_2. The electrical conductivity of A-MnO_2 measured by 4-probe dc conductivity measurements is 1.3×10^{-5} $(\Omega\ cm)^{-1}$. Morphologies from transmission electron microscopy show that A-MnO_2 consists of platelets on the order of 250 Å by 500 Å. Electron diffraction studies do not show long-range order for A-MnO_2, just broad diffuse halos. Far-infrared data for A-MnO_2 show bands at 430, 350, 318, 271, 228, 193, 146, 120, and 84 cm^{-1}. The positions of these peaks and relative intensities are quite different than those for tunnel structure synthetic todorokite (OMS-1) and synthetic cryptomelane (OMS-2). Far-IR spectra for synthetic crystalline birnessite materials are very similar to data for A-MnO_2.

Short-range order of AMO is currently being investigated with X-ray absorption and neutron-scattering methods. Near-edge structure[41] of manganese oxide minerals supposedly can distinguish layer and tunnel structure materials as can NS methods.[42]

IV. Discussion

A. Manganese Complexes and Manganese Oxides. X-ray diffraction data of Figure 2, thermal analyses of Figure 8, FTIR data of Figure 9, and physical and bulk analytical data of Table 1 all suggest that relatively pure samples of amorphous manganese oxides, crystalline commercial manganese oxides, and crystalline oxalatomanganate complexes have been prepared. Photolysis of the oxalatomanganate complexes (as well as oxalato complexes that form to a small extent in amorphous systems) leads to decomposition of the oxalate ligand.

Manganese(3+ or 4+) ions have available d, s, and p orbitals that can form bonds with oxalate ligands. However, potassium oxalatomanganate complexes are photochemically unstable. For our particular syntheses, these complexes are difficult to form because the reaction medium was chosen to be aqueous solution rather than nonaqueous solvents.[22,23,27,28] The possibility that the potassium oxalatomanganate complexes are active photocatalysts instead of manganese oxides is ruled out by photocatalytic data of Table 1.

Although mixed valent manganese(3+ or 4+) oxides like other transition metal oxides[32] are only moderately stable because the valence of the Mn ions and the surface states of the manganese oxides vary with different gaseous atmospheres and temperatures,[33] all manganese oxides (either commercial materials or those prepared by us) were at least partially regenerable under our reaction conditions in an oxygen atmosphere. Crystalline manganese oxides such as todorokite, hollandite, and pyrolusite showed very poor photocatalytic activities (Figure 3). Their three-dimensional network crystal structures probably promote self-quenching of excited manganese ions which are in the framework of these materials. Another reason might be that the large lattice energy of their crystal structures creates a larger energy barrier and minimizes the movement of lattice oxygen from the bulk to the surface of the crystals under the mild reaction conditions of visible light and room temperature that were used in this study. Thus, activation and regeneration of these crystalline catalysts were limited as compared to the amorphous manganese oxide catalysts reported here.

Thermal analysis data of Figure 8 show clear differences between the most active A-MnO_2 and less active commercial crystalline samples. The weight loss temperatures associated with bulk oxygen release[31] are different for the two catalyst systems (A-MnO_2 and commercial MnO_2). The commercial manganese dioxide releases bulk lattice oxygen[22,23,31] at higher temperatures than A-MnO_2. The amount of released bulk oxygen from commercial manganese dioxide is larger than that from A-MnO_2. This is consistent with small structural differences between these two catalysts. The commercial manganese dioxide has low crystallinity, but A-MnO_2 is amorphous. Therefore, the release of oxygen from A-MnO_2 is easier than from the commercial manganese dioxide. The commercial manganese dioxide catalyst needs to absorb a large amount of heat (550 °C) for reduction of Mn^{4+}, releasing the majority of its bulk oxygen and destroying its structure. Reduction of A-MnO_2 is more facile. This difference may be an important factor as to why A-MnO_2 catalysts have higher activity and are more readily regenerated than commercial manganese dioxide.

XRD data for AMO are of very poor resolution. However, the peak near the 2.4-Å d spacing is observed in all octahedrally coordinated manganese oxide materials. The peak near 7.0 Å is also found in most layered materials such as birnessite. Birnessite is the most abundant manganese oxide mineral, and this also lends credence to our belief that AMO is a layered octahedrally coordinated MnO_6 structure type.

Further support for these structural assignments comes from far-infrared data. Oetter and Rossman[44] suggest that natural manganese oxide structure types can be distinguished from each other in the 600–20-cm^{-1} far infrared region of the spectrum. Far-IR data from our labs help eliminate the possibility that AMO is a synthetic amorphous tunnel structure derivative of either cryptomelane or todorokite.

(40) Cao, H.; Chen, J.; Suib, S. L. Manuscript in preparation.
(41) Manceau, A.; Gorshkov, A. I.; Drits, V. A. *Am. Miner.* **1992**, *77*, 1133–1143.
(42) Carrado, K. A.; Thiyagarajan, P.; Winans, R. E.; Botto, R. R. *Inorg Chem.* **1991**, *30*, 794–799.
(43) Wasserman, S.; Carrado, K. A.; Suib, S. L. Unpublished results.

X-ray powder diffraction, FTIR, cyclic voltammetry, electrical conductivity, TEM, ED, and catalytic data[22,23,45] to date suggest that AMO is more like a layered manganese oxide like birnessite than a tunnel structure material like todorokite or hollandite. Further studies in this area with XAS and NS methods are underway.[43]

B. Photocatalysis Studies. It is clear that with flow reactions (Figure 1) of gas-phase 2-propanol that rates of formation (Figure 4) and yields of acetone (Figure 5) are enhanced as power levels are increased. Prephotolyses of all materials (Figure 6) in any atmosphere lead to a decrease in rates and yields of acetone, suggesting that photolysis causes changes in surface intermediates. The valence band XPS data of Figure 7, thermal analysis data of Figure 8, and catalytic data suggest that loss of oxygen from all manganese oxide catalysts limits the overall yield of acetone in these reactions. Rates of alcohol oxidation are slowed down by loss of O_2 and by doing experiments in the absence of oxygen. Amorphous A-MnO_2 catalysts are the most active, selective, and regenerable of any materials we have studied.[22,23] There appears to be little correlation between surface area and activity for catalysts studied here (Table 1).

The main components of amorphous (Figure 2) manganese oxide catalysts are manganese(3+ or 4+) species and oxygen, as determined by XPS, titration, EDX, and bulk analytical experiments (Figure 7, Table 1). Potassium ions counterbalance the reduced Mn^{4+} ions (Mn^{3+}). The multiple oxidation states of these oxides along with their electron donor–acceptor properties make them good oxidation–reduction catalysts that are regenerable.[22,23] The brown color of these amorphous manganese oxides materials allows considerable absorption of visible light.

Infrared spectra (Figure 9) were obtained in an effort to show the presence of hydroxyl groups on MnO_2 samples. Fresh amorphous A-MnO_2 has a broad absorption in the 3600–3100-cm^{-1} range, as shown in Figure 9a. Photolyzed samples of A-MnO_2 also show weak hydroxyl absorptions (Figure 9d). Hydroxyl groups appear to have an important role in photocatalytic reactions because heating the catalyst to 100 °C for 1 h or continually performing photocatalytic reactions at 70 °C leads to a dramatic decrease in activity.

Surface oxygen species on manganese oxides are believed to take part in the decomposition of 2-propanol. The amount of surface oxygen species on the manganese dioxide catalyst that was photolyzed for 30 min measured by in situ XPS methods increased about 5 times (Figure 7). These data suggest that either oxygen migrates to the surface, manganese migrates to the bulk, or both processes occur during photolysis. When the reaction was carried out on manganese dioxide catalysts pretreated in an oxygen-free atmosphere, the amount of acetone formed was observed to be much lower than that from the fresh manganese oxide (Figure 6). Upon illumination, surface oxygen was rapidly lost and bulk oxygen moved to the surface. Light may activate this oxygen release, leading to loss of catalytic activity if not enough oxygen carrier gas is present to replenish oxygen in the catalysts.

C. The Role of Oxygen Species. Assuming that the main contribution to photocatalytic oxidation by manganese oxide catalysts is the electron transfer and reducibility of manganese, reoxidation of manganese must be considered. Oxygen (as an electron acceptor) obtains a negative charge from the reduced manganese species while it is excited by photons and can regenerate bulk oxygen, leading to regeneration. One adsorbed oxygen molecule can fill two oxygen anion vacancies during catalysis, and the bulk of the catalyst can return to its initial state (via regeneration).

When reactions were carried out under oxygen-free conditions, oxygen is evolved from the manganese oxide materials themselves. As the reaction progresses, bulk oxygen and atmospheric oxygen (present in minute amounts from reactor walls) are exhausted, leading to a loss of activity. Kung[31] has suggested that metal oxides typically evolve oxygen in three stages. At first, adsorbed molecular oxygen is evolved, followed by adsorbed atomic oxygen, and finally lattice oxygen. Temperature programmed desorption data for a variety of metal oxides show a loss between about 30 °C and temperatures above 600 °C, but usually in three stages. Data for commercial MnO_2 suggest loss of oxygen at temperatures as low as 50 °C.

Kon et al.[32,34] and Cunningham et al.[35] have extensively studied the reoxidation of oxides and suggest that it occurs in a sequence of steps. Thus, the sequence of oxygen uptake from atmospheric gas to the surface of a partially reduced manganese oxide catalyst may occur as shown in eq 1: Most of the oxygen radicals are

$$O_2(g) \rightarrow (O_2^-) \rightarrow 2(O^-) \rightarrow O^{2-}(s) \qquad (1)$$

believed to be present in the bulk of the catalyst, and some may remain on the surface for a short period. Such oxygen radicals are very active and may regenerate reduced manganese species as well as catalyze hydrogen abstraction from 2-propanol.

The sequence of oxygen release from MnO_2 catalysts may be due to movement of O^{2-}(bulk) to the surface upon the absorption of light with weakening of MnO_2 bonds. Our photochemical data suggest that excited-state oxygen species, even though their lifetime is very short, play a role in hydrogen abstraction of 2-propanol, due to their high energies and electronegativities. Possible pathways are shown in eq 2(a–c).

$$O^{2-}(s) \xrightarrow[e^-]{h\nu} (O^-) \xrightarrow[e^-]{h\nu} O_2(\text{surface}) \qquad (2a)$$

$$O_2(\text{surface}) + CH_3CH_2OHCH_3 \rightarrow O_2(\text{surface}) - H + {}^{\bullet}COH(CH_3)_2 \qquad (2b)$$

$$O_2(\text{surface}) + {}^{\bullet}COH(CH_3)_2 \rightarrow O_2(\text{surface}) - H + (CH_3)_2CO \qquad (2c)$$

The abstracted hydrogen from the alcohol is believed to be oxidized to form acid sites present on the surface of the manganese oxide catalysts, as evidenced by FTIR data. This process is shown in eq 3:

$$H^{\bullet} \xrightarrow{h\nu} H^+ \qquad (3)$$

The regeneration of catalysts may consist of three elemental steps, as shown in eqs 4–6:

$$-Mn^{(3+\text{ or }2+)}- \underset{h\nu}{\overset{-e}{\rightarrow}} -Mn^{(4+\text{ or }3+)}- \qquad (4)$$

$$O_2(g) \xrightarrow{+e} (O_2^-) \xrightarrow{+e} 2(O^-) \xrightarrow{+e} O^{2-}(s) \qquad (5)$$

$$n(-Mn^{(4+\text{ or }3+)}-) + O^{2-} \rightarrow MnO_2 \text{ (or } Mn_2O_3) \qquad (6)$$

It is clear from photochemical and spectroscopic data shown above that regeneration is a key step as regards high activity in such systems. It appears that amorphous materials like A-MnO_2 are more readily regenerable than crystalline manganese oxide systems. FTIR data show that hydroxyl groups of AMO are lost during photolysis. It may be possible that OH moieties are reactive species that help extract H from the alcohol with formation of water. ^{17}O and ^{18}O labeling studies are being done to pursue this possibility.[40]

A reviewer has questioned implications that lattice oxygen needs to be oxidized to adsorbed molecular O_2 for reaction since O^- can be very important in oxidations. Without labeling studies

(44) Potter, R. M.; Rossman, G. R. *Am. Miner.* **1979**, *64*, 1199–1218.
(45) DeGuzman, R. N.; Shen, Y. F.; Suib, S. L.; Shaw, B. R.; O'Young, C. L. *Chem. Mater.* **1993**, *5*, 1395–1400.

this is difficult to definitely show, however, attempts to observe paramagnetic O^- on AMO and other materials with EPR[40] have been unsuccessful. In addition, loss of oxygen from AMO that is held until desorption at elevated temperature (>300 °C) that is believed to be lattice or bulk oxygen (on the basis of TPD data) leads to total loss of activity. TPD experiments on AMO clearly show that oxygen from the bulk migrates to less energetic surface sites that need to be regenerated to maintain activity.

Such photoassisted catalytic oxidations may play an important role in the areas of environmental catalysis for destruction of toxic hydrocarbon species[36,37] as well as in energy conversion systems such as chemical heat pumps.[38,39] Saito et al.[38,39] have recently shown that 2-propanol to acetone conversion can be carried out thermally at extremely low temperature (80 °C). The cost of such precious metal catalysts to date may be prohibitive for current commercial use.

The systems used by Saito et al.[38,39] show another feature common to systems discussed here. The active precious metal catalyst needs to be dispersed on a carbon support, as our system needs a MgO matrix. The role of the C and MgO supports on such systems is vital but not well understood. Preliminary data[40] from our laboratories suggest for the photochemical systems that the function of MgO is to disperse the active component perhaps for better absorption of light as well as possibly provide synergistic effects as regards bond making and breaking of catalytic intermediates. Selective adsorption of catalytic intermediates on the MgO or at the AMO/MgO interface might also enhance conversion in such systems.

V. Conclusions

We have shown here that a new class of amorphous manganese oxide materials are more active photooxidation catalysts and are more regenerable than crystalline manganese oxides or any other oxidic catalysts that have been studied. The ability of manganese to cycle between various oxidation states (4+, 3+, 2+) and of oxygen to migrate to the surface of the amorphous catalyst with regeneration by atmospheric oxygen during photolysis may hold a key to the design of better photocatalyst systems. The presence of surface hydroxyl groups enhances conversion in such systems. Crystalline mixed valent manganese oxide catalysts are not as active or as regenerable as amorphous materials due to changes in structure during photolysis. Finally, enhanced conversions are possible in such systems when gas phase flow reactions are used rather than slurry batch reactions.

Acknowledgment. The authors thank Xiaozhong Tang for collecting the BET data and William S. Willis for collecting XPS data. We thank the Department of Energy, Office of Basic Energy Science, Division of Chemical Science, for support of this research. Helpful discussions with Dr. James Freihaut of United Technologies Research Center are greatly appreciated.